JOURNAL OF Materials CHEMISTRY

Freeze-dried promoted and unpromoted sulfated zirconia and their catalytic potential

Kulamani Parida,† Veronika Quaschning, Elfriede Lieske and Erhard Kemnitz*

Humboldt-Universität zu Berlin, Hessische Str. 1-2, Berlin D-10115, Germany. E-mail: erhard=kemnitz@chemie.hu-berlin.de

Received 15th November 2000, Accepted 12th April 2001
First published as an Advance Article on the web 29th May 2001

A new synthesis route for sulfated zirconia and iron, manganese, and iron–manganese promoted sulfated zirconia has been investigated. Zirconium hydroxide precursors were prepared from hydrogel and hydro-alcogel; freeze-drying as well as oven-drying has been employed. The pure hydroxides, sulfated, and metal promoted sulfated zirconia were calcined at 650 °C and characterised by chemical analysis, XRD, TG/DTG/DTA, nitrogen adsorption, SEM, FTIR pyridine adsorption, and ammonia TPD. The catalytic activity of the samples was screened in the double bond isomerisation of 1-butene and the benzoylation of anisole.

Significant differences in the textural and acidic properties were found for samples prepared either by freeze- or oven-drying. Virtually no difference in acidity was observed between sulfated and metal promoted sulfated zirconia.

Freeze-drying, especially the hydro-alcogel synthesis, was found to be a powerful preparation method for promoted and unpromoted sulfated zirconia catalysts.

Introduction

Sulfated zirconia (SZ) based solid acid catalysts have been highlighted by many research groups as potentially viable substitutes for currently used liquid acids such as HF, H_2SO_4, and chlorinated alumina catalysts.[1–10] Initially, SZ was considered to be a superacid, *i.e.* exhibiting an acidity stronger than that of 100% sulfuric acid.[11–14] However, this point of view has been contradicted by many groups.[15–19] The non-corrosive acid SZ exhibits a high activity for low-temperature n-butane isomerisation. Low temperature isomerisation is of interest to the petroleum industry as branched alkanes are becoming an important product for use as octane boosters in gasoline. A lower reaction temperature not only represents energy savings, but also thermodynamically favours the desired branched products.[20] The rapid deactivation and lack of regenerability[21–22] has led Hsu *et al.*[23] to develop iron and manganese promoted SZ (FMSZ). These catalysts are capable of isomerising n-butane at near room temperature with rates approximately two or three orders of magnitude greater than SZ.[23–25] Sulfate promoted zirconia has also been shown to be active for a number of other reactions including cracking, alkylation, and esterification.[26–30] Friedel–Crafts acylation such as the reaction between benzoyl chloride and anisole to produce 4- and 2-methoxybenzophenone is of industrial importance for the production of fine chemicals. This kind of reaction is catalysed using both Lewis acids ($AlCl_3$, $FeCl_3$, BF_3, $ZnCl_2$, $TiCl_4$) or Brønsted acids (polyphosphoric acid, HF),[31–33] but SZ can be used successfully as a catalyst, too. Clark and Macquarrie[34] have published general aspects of the use of solid acids in environmental clean technologies.

The activity and selectivity of SZ and FMSZ can be greatly influenced by the methods of preparation of zirconium hydroxide, starting zirconium salt precursor, method of sulfation, promoter concentration and activation treatment *etc.*[25,35–40] It has been suggested by many researchers that a high surface area tetragonal phase is necessary for high catalytic activity.[1,4,6,26,41–44] However, recently, Stichert and Schüth[45] have shown that high surface area monoclinic SZ shows an activity comparable to tetragonal zirconia. Since a high surface area is desirable for high activity, various methods have been adopted to obtain this. Among all the methods of preparation, samples prepared as aerogels[9,30,46] have drawn the attention of many research groups. Aerogels and cryogels prepared by the sol–gel method followed by supercritical and freeze-drying, respectively, are supposed to give high surface area and high porosity materials. However, most attention has been given to the preparation of aerogels. In fact, there have been several attempts to prepare cryogels by freeze-drying, on the assumption that the pore liquid could be frozen and sublimed without generating the capillary forces which destroy the gels during evaporative drying.[47] But in most cases, cryogels usually show damage to the pore structure, leaving cracks or large pores in the dried gel.[48–51] However, Yoshida *et al.*[52] have freeze-dried gels containing water. Cryogel-based alumina and chromia catalysts with aerogel-like properties were synthesised by Kirchnerova *et al.*[53] Su *et al.*[54] reported on nanosize zirconia catalysts, prepared by freeze-drying amongst other techniques. A review article about the cryochemical synthesis of oxidic material was recently published by Tretyakov and Shlyakhtin.[55]

In the present study, we have processed hydrous zirconia prepared from two routes of precipitation, *i.e.* hydrogel and hydro-alcogel, followed by oven-drying as well as freeze-drying for the synthesis of SZ and FMSZ. The aims of our investigation are i) the surface and textural characterisation of zirconium hydroxide, zirconia, and modified zirconia and ii) the determination of the effect of Fe, Mn, and Fe–Mn on the double bond isomerisation of 1-butene and on the benzoylation of anisole. The work on the preparation and characterisation of SZ and FMSZ made by freeze-drying is the first of its kind.

Experimental

Sample preparation

Preparation from zirconium oxychloride (hydrogel). Zirconium hydroxide gel was prepared at RT at a constant pH of

†On leave from: Regional Research Laboratory, Bhubaneswar 751013, India.

10.0 following the procedure of Mercera *et al.*[56] A 0.4 M solution of $ZrOCl_2 \cdot 8H_2O$ and 12.5% aqueous ammonia were added concurrently drop by drop to a stirred aqueous ammonia solution of pH 10.0. The pH of the precipitate was carefully controlled within 0.2 pH units. The precipitate thus formed was aged in the mother liquor overnight, filtered, and washed until free from chloride.

Freeze-drying (series 1). The hydrogel was transferred into the freeze drier, frozen by liquid nitrogen, and dried in the freeze drier chamber for 72 h to yield very light large shiny glass-like particles. At the end of the drying process, the chamber temperature and pressure were −29 °C and 0.11 mbar, respectively. To maintain uniformity in the drying process, the hydroxide was further dried in an oven at 110 °C for 4 h.

Oven-drying (series 2). The hydrogel was dried at 110 °C for 12 h. The shrunken, hard mass thus formed was powdered to less than 100 mesh size and dried at 110 °C for 4 h.

Preparation from a zirconium oxychloride/*tert*-butanol mixture (hydro-alcogel). Equal volumes of zirconium oxychloride (0.4 M) and *tert*-butanol were mixed thoroughly and then added drop by drop to the aqueous ammonia solution of pH 10.0. The precipitate free from chloride anion was suspended in *tert*-butanol, stirred for 2 h and filtered.

Freeze-drying (series 3). The hydro-alcogel was dried in the freeze drier for 72 h. The resulting powder was processed in the same manner as the other freeze-dried sample.

Oven-drying (series 4). The mixture was dried in the oven similar to series 2.

Additionally, a commercial zeolite H-β (Süd-Chemie, Si/Al = 25, $S_{BET} \approx 500\ m^2\ g^{-1}$) was used for comparison as solid acid catalyst in the two investigated reactions.

Preparation of sulfate, iron, and manganese promoted zirconia

Sulfate, iron, and manganese were incorporated into the 110 °C dried zirconium hydroxide samples by incipient wetness impregnation. At first, about 12 g of the hydroxide sample was soaked with 12 ml of a solution containing 1 g ammonium sulfate (decomposed to produce approximately 8 wt% SO_4^{2-}), stirred well, and evaporated to dryness with continued stirring. The sulfated sample was further dried at 120 °C for 4 h. Part of the sulfated zirconia samples was stepwise impregnated with 0.6 M $Fe(NO_3)_3$ and 0.3 M $Mn(NO_3)_2$ so as to make 1.5 wt% Fe, 0.5 wt% Mn, and 1.5 wt% Fe–0.5 wt% Mn samples to obtain the typical values reported for these kinds of catalysts (see ref. 36 and references therein). After each impregnation step the sample was dried at 120 °C for 4 h.

Activation and nomenclature

On the basis of thermoanalytical experiments and according to earlier reports,[10,36] a calcination temperature of 650 °C was chosen. This temperature is particularly necessary in the case of metal ion promoted catalysts in order to guarantee the onset of catalytic activity. Calcination was performed under flowing air in a quartz tube inside a tubular furnace. The sample was heated at a rate of 10 K min^{-1} to the desired temperature, held at this temperature for 3 h and then cooled to RT. Before performing catalytic runs and experiments for the determination of the sample's acidity, the catalysts were pre-treated in air for about 1 h at 500 °C.

The samples were denoted as follows; S = sulfated, F = iron, M = manganese, Z = zirconia, 65 = calcined at 650 °C. For example 1SFMZ65 denotes that the sulfated sample from series 1 is first promoted with Fe, then with Mn and finally calcined at 650 °C.

Sample characterisation

Identification of the crystalline phases was performed using X-ray powder diffraction with CuKα radiation (XRD 7, Rich. Seifert & Co., Freiberg). Sulfur and carbon contents were determined by elemental analysis. Nitrogen adsorption experiments were carried out at 77 K with an ASAP 2010, Micromeritics, instrument to determine the BET specific surface area and the pore size distribution according to the Barrett–Joyner–Halenda (BJH) method.[57–59] Thermogravimetry, differential thermogravimetry, and differential thermal analysis were performed on a NETZSCH STA 429 system (heating rate: 5 K min^{-1}, end temperature: 1000 °C, flowing air, 40 ml min^{-1}, reference material: α-Al_2O_3). The morphology of differently synthesised FMSZ-samples was observed by scanning electron microscopy (SEM) using a Stereo scan S 360, Cambridge Instruments, operated at 20 kV and 10 mA. The crystallites were separated manually with a brush, transferred to an adhesive tape, then gold was sputtered onto the surface (film thickness about 30–50 nm).

Lewis acid sites (LC) and Brønsted acid sites (BC) were detected semi-quantitatively by FTIR photoacoustic spectroscopy with pyridine (Pyr-PAS), the procedure is described in ref. 30. Briefly, pyridine was adsorbed at 150 °C, and the FTIR spectra of pyridine loaded and unloaded (= background) samples were taken at RT in the range 4000–400 cm^{-1} using a MTEC-cell, FTIR system 2000, Perkin-Elmer instrument. The intensities of the bands at about 1445 cm^{-1} (LC) and 1490 cm^{-1} (LC + BC) in the normalised spectra were used to determine the acidity semi-quantitatively.

Temperature programmed desorption of ammonia (NH_3-TPD) was carried out to characterise the acid strength distribution of some selected samples. Briefly, ammonia was adsorbed at 120 °C onto the surface of the pelleted, pre-treated samples. The TPD program (10 K min^{-1} up to 500 °C) was accompanied by IR-detection (FTIR system 2000, Perkin-Elmer), and the band at 930 cm^{-1} in the spectra was used to continuously monitor the desorption of ammonia. The amount of acid sites was determined by absorption in sulfuric acid and titration.[30]

Catalytic reactions

I. Double-bond isomerisation of 1-butene. Butene isomerisation was performed in a downward-flow, fixed-bed glass reactor. Equal volumes (150–500 mg) of the pelleted calcined catalyst (0.4–0.5 mm diameter fraction) were exposed to the feed stream mixture of nitrogen (10 ml min^{-1}) and 1-butene (0.6 ml min^{-1}) at a temperature of 60 °C. On-line gas chromatography (Shimadzu GC-14A, FID, column: Di-n-propylsulfone on 0.2–0.4 mm Poralith, ID 2.4 mm, length 4 m) was used to determine the composition of the reaction mixture consisting of 1-butene and *cis*/*trans*-2-butene after 10, 30, 50, 70, 90 min time-on-stream (TOS). Conversion is given as the conversion into the product 2-butene. The catalytic runs were found to be reproducible with an error of less than 5%.

II. Benzoylation of anisole. The acylation reaction between anisole and benzoyl chloride was carried out in a 50 ml three necked round bottom flask fitted with a thermometer, reflux condenser with $CaCl_2$ tube and a magnetic stirrer bar. A mixture of 12 ml anisole and 2.65 mmol of benzoyl chloride was added to the flask along with 0.1 g of n-tridecane which was used as an internal standard for GC. The catalyst was added after adjusting the temperature to 60 °C. The reaction mixture was separated from the catalyst after 3 h and analysed gas chromatographically, using a HP 5890 A (FID, column:

Rtx 1, methylsilicon, Restec corp., ID 0.25 mm, length 30 m). Conversion is given as the conversion into the products, *para*- and *ortho*-methoxybenzophenone; benzoic acid and phenyl benzoate were the only by-products. The influence of reaction temperature was studied on the 3SZ65 sample at 40, 60, 80, and 100 °C. The measurements were reproducible within an error domain of 5%.

Results and discussion

1. Elemental analysis, crystalline phases and microscopy

Elemental analysis and textural characterisation were performed with all samples (zirconium hydroxides and calcined zirconia), data are given in Table 1.

It is evident from elemental analysis that the cryogel samples (series 1 and 3) dried at 110 °C contain a higher percentage of carbon impurities compared with the samples prepared by oven-drying (series 2 and 4). After calcination, the amount of carbon in the modified samples is in the range of 0.1 to 0.2 wt%, thus excluding any negative effect on the catalytic activity. The loss of carbon is more efficient in the presence of sulfur and, as a result, all sulfated samples contain a lower amount of carbon compared to the unpromoted samples.

Although all the samples were impregnated with the same amount of $(NH_4)_2SO_4$ (8 wt% SO_4^{2-}/2.67 wt% S, respectively), the obtained sulfur contents vary for different series. From preliminary TG-MS experiments we can exclude that this effect was due to differences in the mass loss of zirconia precursors during the calcination step. Unmodified zirconia materials from hydrogel as well as hydro-alcogel yielded almost the same mass loss, 14.5% and 13.2%, respectively. Therefore, the nominal S/Zr ratio was the same for all series and final differences in the sulfur contents of the samples are ascribed to textural effects which in turn strongly depend on the method of synthesis. For all the samples of one series, the S content varies after calcination at 650 °C with the promoting elements. In each series, unpromoted SZ has the lowest value, and the sulfur contents increase after impregnation with manganese, iron and even more after impregnation with both promoters. The presence of Fe, Mn, and Fe–Mn might inhibit the loss of sulfur from the surface and shift the sulfur evolution to higher temperatures. Although the obtained sulfur contents are lower than the proposed theoretical monolayer capacity—less than 16.6×10^{-5} g_S m^{-2} compared to 21×10^{-5} g_S m^{-2} [60]—the sulfate contents vary significantly with the specific surface area. For example, sample 3SZ65 (132 m^2 g^{-1}) retained the highest amount of sulfur (1.65 wt%) whereas sample 1SZ65 (69 m^2 g^{-1}) withheld only 1.03 wt% (*cf.* Fig. 1).

Unpromoted hydrous zirconia crystallised as mixtures of monoclinic and tetragonal phases after calcination at

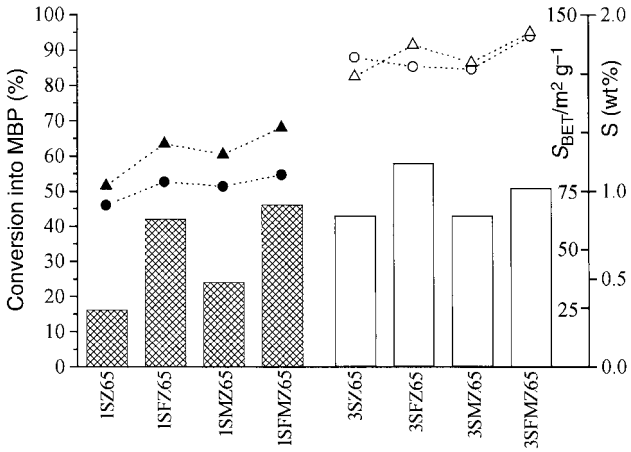

Fig. 1 Influence of the synthesis route on sulfur content (triangles), specific surface areas (circles), and the formation of methoxybenzophenone (MBP, columns) for modified zirconia samples of series 1 (freeze-drying, hydrogel) and 3 (freeze-drying, hydro-alcogel).

Table 1 Physico-chemical characterisation and acid properties of zirconia samples, prepared by different methods. For each series,[a] the 110 °C dried zirconium hydroxide and the modified samples, calcined at 650 °C are presented

Sample	XRD pattern[b]	S/wt%	C/wt%	S_{BET}/m^2 g^{-1}	$V_{P,Des}$/cm^3	d_{max}/Å	BC per unit mass[c]/arb. units g^{-1}	LC per unit mass[c] /arb. units g^{-1}
1	A	—	3.11	174	0.34	200	—	—
1Z65	M	—	0.16	34	0.23	300	—	—
1SZ65	M (T)	1.03	0.14	69	0.27	200	0.14	0.08
1SFZ65	T	1.27	0.17	79	0.24	200	0.15	0.08
1SMZ65	T	1.21	0.16	77	0.26	200	0.15	0.07
1SFMZ65	T	1.36	0.05	82	0.26	200	0.15	0.07
2	A	—	0.86	283	0.14	<20	—	—
2Z65	T (M)	—	0.18	70	0.08	38	—	—
2SZ65	T	1.24	0.09	95	0.10	38	0.13	0.10
2SFZ65	T	1.41	0.10	106	0.11	38	0.13	0.10
2SMZ65	T	1.33	0.07	87	0.10	38	0.11	0.09
2SFMZ65	T	1.45	0.09	99	0.10	38	0.11	0.09
3	A	—	3.35	314	1.22	500	—	—
3Z65	M (T)	—	0.39	81	0.67	500	—	—
3SZ65	T	1.65	0.17	132	0.54	140	0.19	0.09
3SFZ65	T	1.83	0.10	128	0.52	180	0.19	0.09
3SMZ65	T	1.73	0.19	127	0.55	180	0.19	0.13
3SFMZ65	T	1.90	0.03	141	0.58	180	0.19	0.09
4	A	—	1.30	277	0.27	40	—	—
4Z65	M (T)	—	0.14	75	0.16	70	—	—
4SZ65	T	1.20	0.11	93	0.16	53	0.16	0.11
4SFZ65	T	1.37	0.07	105	0.15	45	0.16	0.11
4SFMZ65	T	1.48	0.08	99	0.16	50	0.16	0.11

[a]Series 1: hydrogel, freeze-drying; series 2: hydrogel, oven-drying; series 3: hydro-alcogel, freeze-drying; series 4: hydro-alcogel, oven-drying. [b]A: Amorphous, T: tetragonal zirconia, M: monoclinic zirconia. [c]BC = Brønsted acid sites, LC = Lewis acid sites. No data are given for pure zirconia, since these samples possess Lewis acidity only (*cf.* Fig. 4 and refs. 7, 30 and 61).

650 °C. With the exception of sample 1SZ65, all the calcined impregnated samples possessed only tetragonal phase zirconia. Sulfate, iron, and manganese promotion has been found to inhibit the sintering and surface area decrease upon heat treatment at 650 °C. As observed by others, the presence of sulfate prevents a collapse of the surface network and results in tetragonal phase stabilisation and larger surface areas, whereas pure zirconia hydrogel gives monoclinic and tetragonal zirconia with a comparatively low surface area after calcination at 650 °C. An increase of the zirconia surface area with the addition of modifiers is commonly seen with both sulfate[3,4,6,61–63] and other additives.[64–66]

Comparing the line broadening of the XRD peaks (patterns not shown here), it is obvious that the freeze-dried samples are somewhat less crystalline compared to oven-dried samples.

SEM photographs of samples prepared by different methods show different morphologies (Fig. 2). The samples can be roughly divided into two groups based on their topology and the drying mode. It is clearly seen from the SEM photographs that freeze-dried samples possess rough, rugged surfaces. In contrast, the surface of the oven-dried samples is much smoother and only some upgrowths and agglomeration were observed. Freeze-drying also resulted in smaller particle sizes compared to the oven-dried samples; the cryo-samples are smaller than 10 μm on average.

2. Thermal analysis

Since strong acidity is generated after thermal treatment only, TG, DTG and DTA of impregnated hydro-alcogel samples were used to obtain detailed information on the evolution of species and of the optimal calcination temperature. Profiles of the impregnated samples of series 4 dried at 110 °C were measured, the results for 4S and 4SF are illustrated in Fig. 3. The TG/DTG/DTA curves show characteristics similar to those reported by Figueras *et al.*[10,60] The whole temperature range can be divided roughly into four parts: I. dehydration and dehydroxylation, II. decomposition of organic residue, III. decomposition of the modifiers, accompanied by the formation of chemical bonds to the zirconia surface, crystallisation, and rearrangement, and IV. sulfate decomposition.

I. For all samples, the first endothermic process is spread over a broad temperature range exhibiting a maximum at about 110 °C and a weight loss of 6–10%. This is ascribed to the evolution of water.

II. A second process can be observed at 220–270 °C related to a weight loss of 5–8%. This region is characterised by a strong exothermic oxidation of the organic residue originating from the synthesis with *tert*-butanol. This observation is similar to the report of Figueras *et al.*[10] and was reconfirmed by our TG-MS experiments. For all the metal promoted samples the second process is rather distinct and, consequently, sharp DTG peaks can be observed.

III. The third stage includes the decomposition of ammonium sulfate and, if present, metal nitrates as well as the formation of sulfate bonds and metal containing species. As a result, the curve shape is rather unspecific and only shows a feature at about 450 °C where a small weight loss can be observed in the case of metal ion modification. At 550–580 °C, an exothermic DTA peak occurs; in the case of promoted SZ it is sharper and shifted to higher temperatures. This might be due to the crystallisation of zirconia into the tetragonal phase and should be closely related to the transition of sulfate from a low temperature form to the active high temperature form (surface sulfate),[9] although the crystallisation process is not

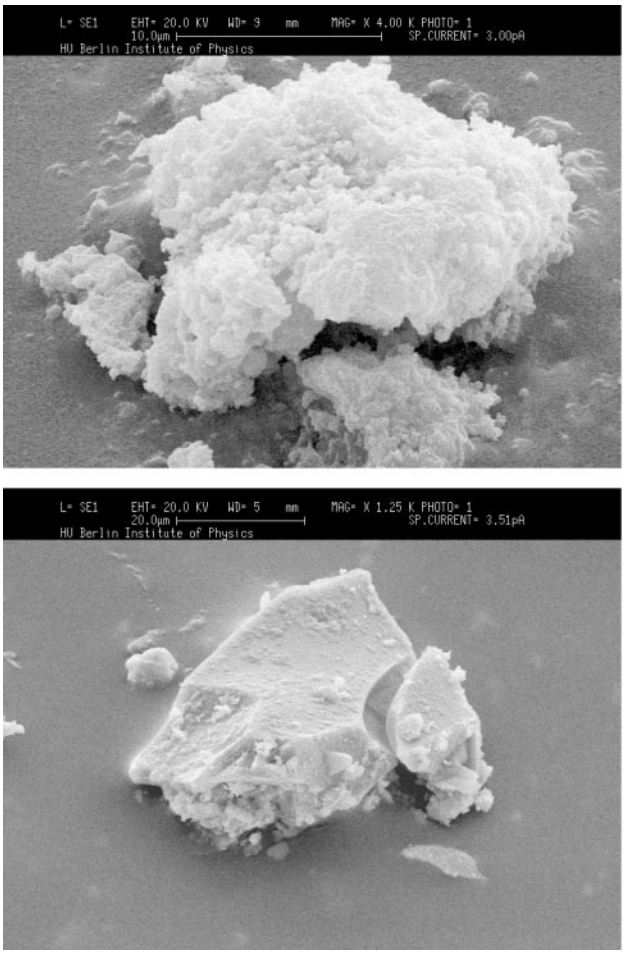

Fig. 2 SEM photographs of calcined SFMZ samples: 3SFMZ65, prepared by freeze-drying (top) and 4SFMZ65, prepared by oven-drying (bottom).

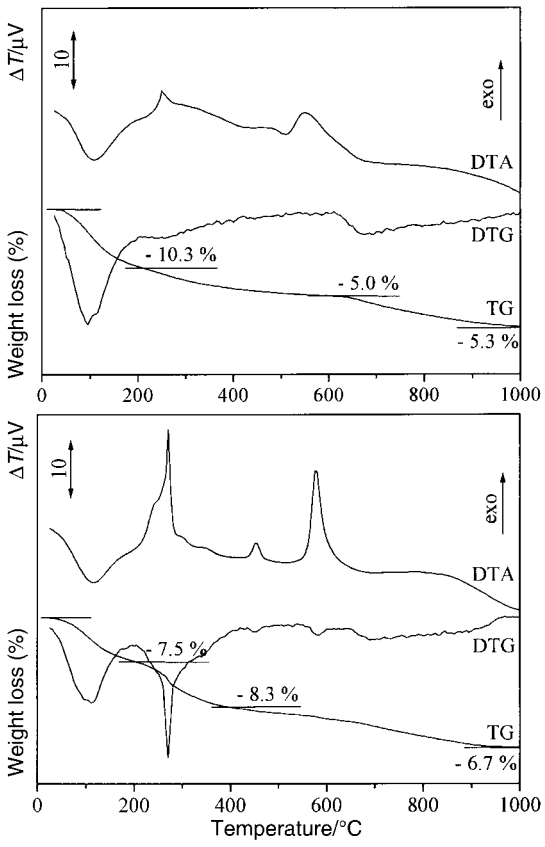

Fig. 3 TG/DTG/DTA profiles of hydro-alcogel samples from series 4 dried at 110 °C, impregnated with sulfate only (top) and sulfate and iron (bottom).

always detectable by DTA or is overlapped by endothermic decomposition processes.[60]

IV. The fourth stage in the TG curve begins at about 610 °C in sulfated samples and 650 °C in Fe–Mn promoted SZ samples. It is related to the sulfate decomposition.

In conclusion, a calcination temperature in the range of 650 °C (=sulfate decomposition) is necessary for this synthesis route, too, to activate the metal promoted SZ.[10,38,39] Although thermoanalytical investigations were only performed for series 4, the same calcination temperature of 650 °C has been chosen for all batches.

3. Pore structure

Nitrogen adsorption/desorption isotherms were measured for all the freeze-dried and oven-dried samples, the most important textural results are given in Table 1. It is evident that the porous structure of hydrous zirconia is not temperature resistant; the initially high specific surface area and pore size decreased markedly on increasing the calcination temperature for all series. In the presence of modifiers, the change in the surface area and pore structure is suppressed.

Varying synthesis routes resulted in large differences in the network structure, some representative pore size distributions, calculated from the desorption branch of the isotherms according to the BJH equation, are shown in Fig. 4. The adsorption isotherms of oven-dried samples (series 2 and 4) were of type IV. The hysteresis loop, associated with capillary condensation in mesoporous structures (pore width between 20 and 500 Å), can be ascribed here to the type H2. However, the shape of pores and the pore size distribution are not well-defined in such systems, formerly it was ascribed to pores with narrow necks and wide bodies.[59] Samples prepared by freeze-drying (series 1 and 3) showed adsorption/desorption isotherms of type II at all temperatures. The hysteresis loop resembled the H3 type according to IUPAC nomenclature. Such loops do not exhibit any limiting adsorption at high P/P_o and are associated with aggregates of plate-like particles giving rise to slit-shaped pores.

Although all the samples were mesoporous, the pore size distribution curves for samples obtained *via* different synthesis methods clearly possessed differences in pore diameter: Oven-dried samples showed a sharp distribution, the structural pores were centered at about 35 (series 2) to 50 Å (series 4). For freeze-dried samples, a broad distribution of pore diameter obtained from the packing of the particles was observed, localised at about 180 (series 3) to 200 Å (series 1). The samples prepared by freeze-drying always possessed a higher pore volume compared to their counterparts prepared by oven-drying, although no clear cut trend is present in the specific surface area values.

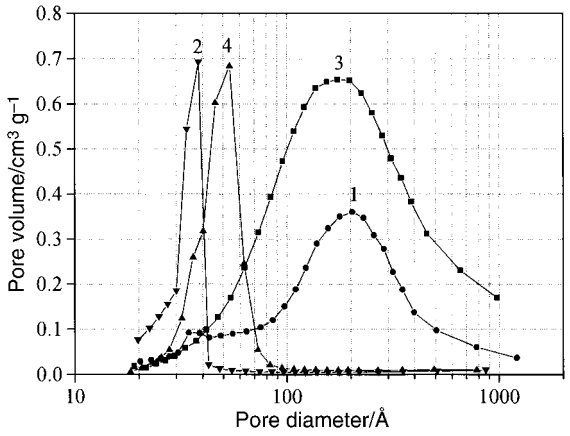

Fig. 4 Pore size distribution of differently prepared zirconia samples, calculated from the desorption branch of the N_2 adsorption isotherms. 1=1SFMZ65, 2=2SFMZ65, 3=3SFMZ65, 4=4SFMZ65.

The highest values of pore volume (>0.5 cm^3 g^{-1}), BJH pore diameter ($\sim$180 Å) and specific surface area ($\sim$130 m^2 g^{-1}) were observed with the samples of series 3, prepared by hydroalcogel and freeze-drying. These textural properties closely resemble the aerogel samples where the network structure is—by means of supercritical drying—also well preserved.

4. Acidic properties from pyridine adsorption and ammonia TPD

With pyridine adsorption, a distinction between Brønsted and Lewis acid sites is possible. The bands at 1445 and 1610 cm^{-1} correspond to different modes of vibration of pyridine co-ordinated to Lewis acid sites (LC), the bands at 1540 and 1640 cm^{-1} have been assigned to the pyridinium ion (Brønsted acid sites, BC). Finally, the band at 1490 cm^{-1} is characteristic for both LC and BC. Semiquantitative values of Brønsted and Lewis acidity determined from the peak intensities at 1445 and 1490 cm^{-1} after correction were collected in Table 1. Since wide differences were observed in the amount of sample needed to fill the photoacoustic sample holder (density varies strongly with synthesis method), these acidity values are given per unit mass. Selected FTIR photoacoustic spectra of pyridine adsorbed on the calcined catalysts are shown in Fig. 5. Unmodified samples contain only LC.[7,30,67] Sulfur treatment leads to the formation of Brønsted acidity. As a result, all the sulfated and metal ion promoted SZ contain both LC and BC. Independent of the presence of promoters, the quantities of BC and LC within the series are similar. Between different series no large differences were observed after mass normalisation. Only slightly higher values for Brønsted acidity were found for series 3, which also possesses the highest specific surface areas.

Temperature-programmed desorption (TPD) of ammonia is a common method for investigating both the strength and number of acid sites present on the surface of an acidic solid. Characteristic profiles of some representative samples of series 3 are presented in Fig. 6. The area under the TPD-curve corresponds to the mass normalised amount of desorbed NH_3 (*cf.* Table 2), which varies proportionally to the specific surface area of the sample. For series 3, the total number of acid sites is the highest. Accordingly after S_{BET} normalisation, the specific concentration of acid sites is more or less the same for all series. As expected, the profile of unmodified zirconia showed only one maximum in the low-temperature region, whereas from the sulfated as well as promoted sulfated samples ammonia could still be desorbed at 500 °C. By separating the TPD-profiles into several temperature sections, as has been done in Fig. 6, it is seen that the main differences between 3SZ65 and 3SFMZ65 on the one hand and 3Z65 on the other arise in the higher temperature region. Since the former samples are significantly more active, it seems that sites in this temperature region are mainly responsible for the catalytic

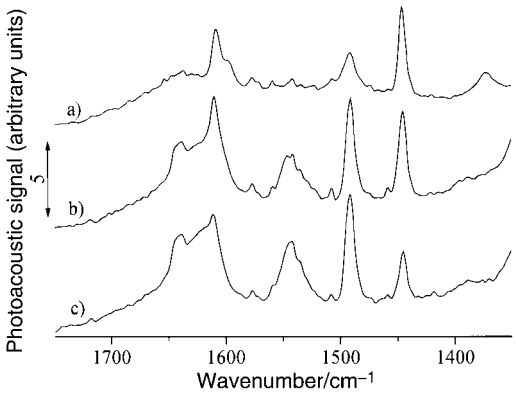

Fig. 5 Normalised FTIR photoacoustic spectra of pyridine adsorbed at 150 °C on zirconia samples: a) 3Z65, b) 3SZ65, c) 3SFMZ65.

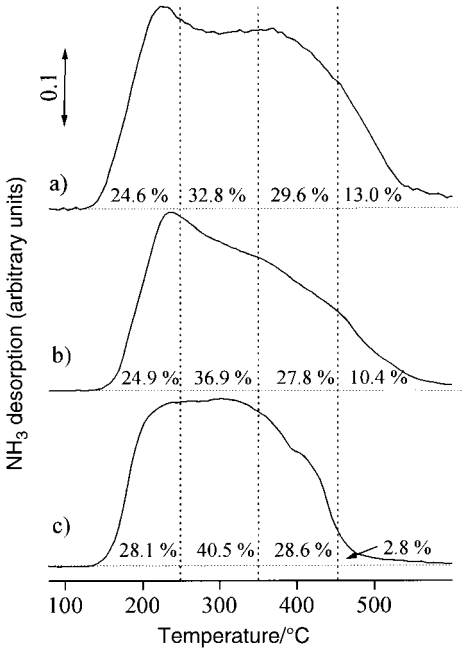

Fig. 6 Temperature-programmed desorption of ammonia on selected samples. Conditions: $m_{sample}=200$–300 mg, $\theta_{ads}=120$ °C, $\theta_{des}=80$–500 °C, flow rate = 10 K min^{-1}. a) 3SZ65, b) 3SFMZ65, c) 3Z65.

action. Thus the catalytic behaviour of the different samples is mainly ascribed to a medium to strong acidity but not to their total concentration which is nearly the same for all samples.

Qualitatively, the same characteristic profiles were obtained for all modified zirconia samples. The presence of iron and/or manganese did not result in a further increase in the acidity, hence, no change in the resulting profile was observed for metal promoted samples. The density of acid sites is 2.4 to 2.6 μmol m^{-2}, similar for all the SFZ65 samples and the specific acidity varies with S_{BET} from 0.20 (series 1) to 0.34 mmol g^{-1} (series 3). Within one series, ammonia desorption was about 0.3 to 0.4 mmol g^{-1} (3.7 to 2.1 μmol m^{-2}), thus metal promoted samples did not show any increase in the amount of acidic sites.

The results from pyridine FTIR and ammonia TPD correspond well to other reports on the acidity of unpromoted and promoted zirconia samples:[17,25,30,67] In contrast to pure zirconia, the addition of sulfate leads to the generation of Brønsted acidity and shifts the maximum of NH_3 desorption to higher temperatures. As proposed by many groups, no further increase in acidity was observed for the metal ion promoted samples.[25,68,69]

5. Catalytic properties

I. Double bond isomerisation of 1-butene. It has been reported by Thomson *et al.*[70] and Tung and McInich[71] that the double bond isomerisation of 1-butene at temperatures below 200 °C occurs exclusively at Brønsted acid sites and above this temperature predominantly at Lewis acid sites.

Table 2 Results from ammonia TPD on selected zirconia samples. Conditions: $\theta_{ads}=120$ °C, $\theta_{des}=80$–500 °C, flow rate = 10 K min^{-1}

Sample	mmol g^{-1}	μmol m^{-2}
1SFZ65	0.20	2.54
2SFZ65	0.25	2.40
3SFZ65	0.34	2.63
4SFZ65	0.24	2.66
3Z65	0.30	3.69
3SZ65	0.41	3.14
3SFMZ65	0.30	2.13

Hence, this reaction may be used to screen qualitatively Brønsted surface sites as has been used *e.g.* by Gao and Moffat[72] to prove Brønsted sites at boron phosphates. In our case, the reaction was performed at 60 °C using equal volumes of catalyst. At such low temperature, *cis*- and *trans*-2-butene were the only products, no skeletal isomerisation or alkylation took place. The mechanism proceeds *via* carbocations, formed by protonation of 1-butene on BC and followed by rearrangement. Table 3 shows the yield of 2-butene after 30 min TOS, the amount of pelleted catalyst used for the reaction, and additionally the conversion into 2-butene normalised to the mass of catalyst. Whatever the preparation procedure and activation temperature, unmodified zirconia was catalytically inactive whereas all the SZ samples were active for this isomerisation. This result corresponds well with data from the literature.[30,61] The ratio of *cis*-/*trans*-2-butene changed with TOS. At the beginning of the reaction it was about 1 : 2, but at higher TOS both isomers were formed in approximately the same scale. This observation fits our former results.

The yield of 2-butene depended strongly on the synthesis route. For equal volumes of the calcined catalysts the order is $2\sim4>3\sim1$, the highest activities of the oven-dried samples are due to higher bulk densities. However, after normalisation onto the mass of catalyst or its surface area this order shifts and becomes $3\sim4>1\sim2$, demonstrating the superior properties of the hydro-alcogel synthesis. The normalised conversion fits well to the observed order of Brønsted acidity and highest values were observed for series 3 (hydro-alcogel and freeze-drying).

All the catalysts promoted with iron and, even slightly more, with iron and manganese were more active than unpromoted SZ. On the other hand, catalysts promoted with Mn only were, surprisingly, even less active than unpromoted SZ. With all the promoted samples calcined at 650 °C rapid deactivation was observed at this low reaction temperature (Fig. 7). Interestingly, deactivation profiles of 1-butene isomerisation were obtained similarly to n-butane isomerisation. This behaviour is in good agreement with the report of Lange *et al.*,[16] showing that Fe and Mn have different deactivation profiles with manganese deactivating particularly rapidly.

Promoted and unpromoted SZ samples exhibited about the same level of Brønsted acidity (after taking the experimental error into consideration), but showed differences in the catalytic performance. Previously it was reported and confirmed by several groups[23,24,73] that metal ion promotion resulted in an increased activity in the conversion of n-butane to isobutane. Now there is an emerging consensus that Fe, Mn and some other promoters do not increase the acid strength on the surface of the catalyst.[17,25,68,69,74] The improvement in activity has been ascribed not to a higher acidity but to the redox capability of these elements, which results in a better initialisation of the reaction of paraffinic to olefinic species. It is interesting to note that we observed the same promoting effect of Fe and Fe–Mn in the isomerisation of an alkene, too.

The mechanism of 1-butene isomerisation on promoted SZ samples might be explained according to the hypothesis of Coelho *et al.*,[74] similar to n-butane isomerisation: In summary, the acid sites are responsible for the formation of carbenium ions whereas redox active sites attract butene molecules to form an olefin pool that enhances the surface concentration near the acid sites.

II. Benzoylation of anisole. The results of the reaction between benzoyl chloride and anisole (eqn. 1), carried out in the liquid phase at 60 °C, are summarised in Table 3. Beside the ketones, benzoic acid and phenyl benzoate were formed as side-products (*cf.* eqns. 2*a* and 2*b*). The ratio of the main products, *para*- and *ortho*-methoxybenzophenone (MBP), is in the range of 95% to 5%, similar observations were made in the case of a homogeneously catalysed benzoylation.

Table 3 Catalytic activities of promoted and unpromoted SZ samples. Butene isomerisation: $\theta = 60\,^{\circ}C$, $N_2 = 10.0$ ml min^{-1}, 1-butene = 0.6 ml min^{-1}, $\tau = 1.2$ s; Acylation: $\theta = 60\,^{\circ}C$, $t = 3$ h, 12 ml anisole, 372.5 mg (2.65 mmol) benzoyl chloride, 0.1 g n-tridecane, 200 mg catalyst

	Butene isomerisation at 60 °C after 30 min TOS			Benzoylation of anisole at 60 °C after 3 h reaction	
Sample	Mass of catalyst/mg	Conversion (%)	Conversion/mass (% mg^{-1})	Conversion (%)	ΣMBP (%)
1SZ65	219	20	0.09	35	16
1SFZ65	225	27	0.12	56	42
1SMZ65	201	14	0.07	37	24
1SFMZ65	289	43	0.15	58	46
2SZ65	335	37	0.11	42	33
2SFZ65	505	51	0.10	63	51
2SMZ65	348	30	0.09	41	20
2SFMZ65	350	62	0.18	56	42
3SZ65	139	25	0.18	53	43
3SFZ65	215	35	0.16	68	58
3SMZ65	125	14	0.11	56	43
3SFMZ65	140	30	0.21	69	51
4SZ65	264	43	0.16	43	36
4SFZ65	382	56	0.15	62	43
4SFMZ65	275	62	0.23	61	45
Zeolite H-β	71	5.7	0.08	33	6

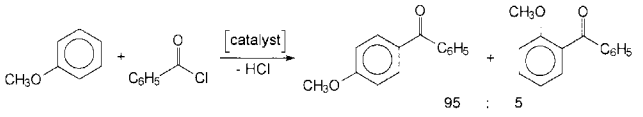

(1)

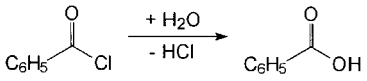

(2*a*)

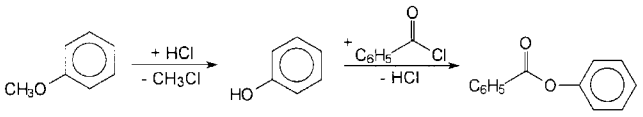

(2*b*)

Again, pure zirconia samples are—similar to the double bond isomerisation—catalytically inactive for the acylation reaction and all modified samples possess good acylation activity and a selectivity to methoxybenzophenone of about 65–85%. Samples from series 3, prepared by hydro-alcogel synthesis and freeze-drying, were the most active catalysts. Comparing the different synthesis series, the order of activity is $3 > 2 \sim 4 > 1$. This is in very good agreement with the surface areas of these samples. In contrast to the butene isomerisation, the same mass of catalyst was used for these experiments, and the active surface area was in the same order: $3 > 2 > 1 \sim 4$.

Compared to unpromoted SZ, the conversion and selectivity increased in the case of iron promoted samples, no such effect was observed for Mn promoted samples. A promoting effect of iron in montmorillonite and vermiculite on Friedel–Crafts alkylation and nitration reactions, respectively, was also reported by others.[75,76] Similar to the proposed model of the butene isomerisation, the cycle of the Friedel–Crafts acylation between benzoyl chloride and anisole is proposed to incorporate both metal ions as redox sites (to attract the reactants) and Brønsted acid sites (for the intrinsic catalytic step). At the BC, cationic species are formed from the pool of reactants by protonation; these benzoyl cations will give the ketone *via* an electrophilic attack of the aromatic anisole, preferentially in the *para*- and *ortho*-positions.

The dependence of the degree of conversion on the reaction temperature was investigated for the sample 3SZ65 and is given in Fig. 8. SZ is able to catalyse the benzoylation of anisole at lower reaction temperatures, too. The activity and the yield of 4-methoxybenzophenone increased considerably with an increase in the reaction temperature from 40 to 100 °C. The higher selectivity to the ketone is ascribed to a reduced formation of benzoic acid when the reaction is performed at higher temperatures.

The commercial zeolite H-β was additionally tested under the same conditions as a reference (Table 3). Butene isomerisation after 30 min TOS yielded only 6% conversion into 2-butene, even the mass normalised conversion did not exceed 0.08% mg^{-1}. In the benzoylation of anisole, the degree of conversion and selectivities were much lower in the case of the zeolite (33% and 18%, respectively) compared to all the SZ samples. Although zeolite H-β is known for its very

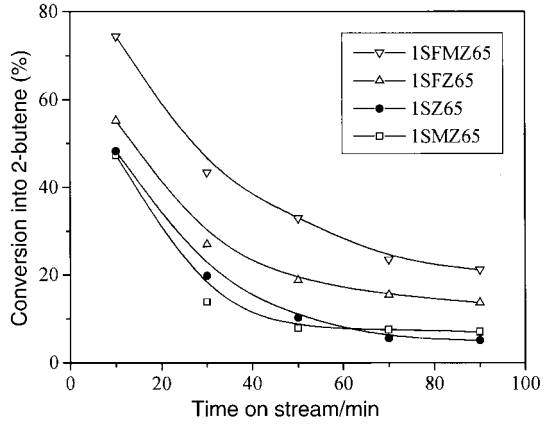

Fig. 7 Effect of TOS on the conversion of 1-butene for different modified zirconia samples. Conditions: $N_2 = 10$ ml min^{-1}, 1-butene = 0.6 ml min^{-1}, $m_{catalyst} = 200$–300 mg, $\tau = 1.2$ s, $\theta_{reaction} = 60\,^{\circ}C$.

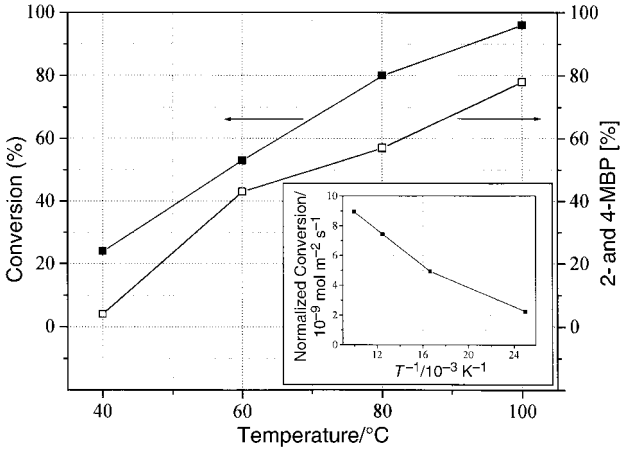

Fig. 8 Benzoylation of anisole: effect of the temperature on the conversions and yields of methoxybenzophenone after 3 h reaction time. Conditions: 12 ml anisole; 372.5 mg (2.65 mmol) benzoyl chloride; 100 mg n-tridecane; 200 mg catalyst (3SZ65).

good acylation activity,[77] only a 6% yield of methoxybenzophenone was obtained after 3 h reaction time. Therefore, it can be concluded that under these mild reaction conditions SZ is a much more suitable catalyst for this type of reaction, especially in the case of an improved synthesis route (hydrogel-alcogel, freeze-drying, metal ion promoters).

Conclusions

(1) Promoted and unpromoted SZ with comparatively high surface areas and acidities have been synthesised from a hydro-alcogel mixture (series 3) prepared by freeze-drying. All the samples prepared by freeze-drying possessed higher pore volumes and pore diameters than samples prepared by the conventional oven-drying process. The latter samples exhibited a narrow pore size distribution with a maximum in the range of 30–50 Å. The high mesoporosity in the cryo-samples is due to inter-particulate voids. Therefore, freeze-drying, especially starting from hydro-alcogels, was established as a potential method for the synthesis of aerogel-like SZ materials.

(2) The retention of sulfur in sulfated and metal promoted sulfated zirconia at 650 °C depends on the surface area of the support (sulfate–support interaction), the presence of promoters is an advantage.

(3) A high catalytic activity of the metal ion promoted SZ in the isomerisation of 1-butene and in the acylation was observed and might be due to a synergism between acid and redox properties. The metal ion sites are proposed to interact strongly with the reactants, therefore a higher concentration of reactants is present near the Brønsted acid sites which are involved in the catalytic step.

(4) All the modified zirconia samples gave comparatively high conversions for the benzoylation of anisole, superior to those obtained using a zeolite H-β catalyst. The reaction strongly depends on the temperature; sample 3SZ65 showed 96% conversion and 81% yield of ketone at 100 °C (*cf.* Fig. 8), thus making these catalysts attractive for this kind of reaction.

Acknowledgements

K. P. is thankful to the DAAD and CSIR for sponsoring his visit to Germany. We also thank H. Prescott for her help in freeze-drying as well as Dr G. Kauschka and Dr S. Rogaschewski for taking the SEM images. This study was supported by the Fonds der Chemischen Industrie (FCI grant) and the Bundesministerium für Bildung, Wissenschaft, Forschung und Technologie (BMBF: FKZ 03C0275A).

References

1 (*a*) M. Hino, S. Kobayashi and K. Arata, *J. Am. Chem. Soc.*, 1979, **101**, 6439; (*b*) M. Hino and K. Arata, *J. Chem. Soc., Chem. Commun.*, 1980, 851.
2 B. H. Davis, R. A. Keogh and R. Srinivasan, *Catal. Today*, 1994, **20**, 259.
3 R. Srinivasan, D. Taulbee and B. H. Davis, *Catal. Lett.*, 1991, **9**, 1.
4 J. M. Parera, *Catal. Today*, 1992, **15**, 481.
5 A. Corma and A. Martinez, *Catal. Rev. Sci. Eng.*, 1993, **35**, 483.
6 F. R. Chen, G. Coudurier, J. F. Joly and J. C. Vedrine, *J. Catal.*, 1993, **143**, 616.
7 (*a*) C. Morterra, G. Cerrato, V. Bolis, S. Di Ciero and M. Signoretto, *J. Chem. Soc., Faraday Trans.*, 1997, **93**, 1179; (*b*) C. Morterra, G. Cerrato, F. Pinna, M. Signoretto and G. Strukul, *J. Catal.*, 1994, **149**, 181.
8 A. Sayari and Y. Yang, *J. Catal.*, 1999, **187**, 186.
9 (*a*) D. A. Ward and E. I. Ko, *J. Catal.*, 1994, **150**, 18; (*b*) D. A. Ward and E. I. Ko, *J. Catal.*, 1995, **157**, 321; (*c*) D. A. Ward and E. I. Ko, *Chem. Mater.*, 1993, **5**, 956.
10 K. Biro, F. Figueras, C. M. Alvarez, S. Bekassy and J. Valyon, *J. Therm. Anal. Calorim.*, 1999, **56**, 345.
11 E. Iglesia, S. L. Soled and G. M. Kramer, *J. Catal.*, 1993, **144**, 238.
12 F. Garin, L. Seyfried, P. Girard, G. Maire, A. Abdulsamad and J. Sommer, *J. Catal.*, 1995, **151**, 26.
13 D. Tichit, D. EI Alami and F. Figueras, *J. Catal.*, 1996, **163**, 18.
14 M. Misono and T. Okuhara, *CHEMTECH*, 1993, **23**, 23.
15 V. Adeeva, G. D. Lei and W. M. H. Sachtler, *Appl. Catal.*, 1994, **118**, L11.
16 (*a*) T. K. Cheung, J. L. d'Itri, F. C. Lange and B. C. Gates, *Catal. Lett.*, 1995, **31**, 153; (*b*) T. K. Cheung, J. L. d'Itri and B. C. Gates, *J. Catal.*, 1995, **153**, 344; (*c*) T. K. Cheung, F. C. Lange and B. C. Gates, *J. Catal.*, 1996, **159**, 99; (*d*) F. C. Lange, T. K. Cheung and B. C. Gates, *Catal. Lett.*, 1996, **41**, 95.
17 J. E. Tabora and R. J. Davis, *J. Chem. Soc., Faraday Trans.*, 1995, **91**, 1825.
18 J. Sommer, R. Jost and M. Hachoumy, *Catal. Today*, 1997, **38**, 309.
19 E. Brunner, *Catal. Today*, 1997, **38**, 361.
20 G. A. Olah, G. K. Surya Prakash and J. Sommer, *Superacids*, Wiley, New York, 1985.
21 J. C. Yori, J. C. Luy and J. M. Parera, *Catal. Today*, 1989, **5**, 493.
22 F. Garin, D. Andriamasinoro, A. Abdulsamad and J. Sommer, *J. Catal.*, 1991, **131**, 199.
23 C. Y. Hsu, C. R. Heimbuch, C. T. Armes and B. C. Gates, *J. Chem. Soc., Chem. Commun.*, 1992, 1645.
24 A. Jatia, C. Chang, J. D. MacLeod, T. Okubo and M. E. Davis, *Catal. Lett.*, 1994, **25**, 21.
25 K. T. Wan, C. B. Khouw and M. E. Davis, *J. Catal.*, 1996, **158**, 311.
26 K. Arata, *Adv. Catal.*, 1990, **37**, 165.
27 S. Ardizzone, C. L. Bianchi, V. Ragaini and B. Vercelli, *Catal. Lett.*, 1999, **62**, 59.
28 K. M. Parida and P. K. Pattnayak, *Catal. Lett.*, 1997, **47**, 255.
29 Y. Xia, W. Hua and Z. Gao, *Catal. Lett.*, 1998, **55**, 101.
30 V. Quaschning, J. Deutsch, P. Druska, H. J. Niclas and E. Kemnitz, *J. Catal.*, 1998, **177**, 164.
31 G. Merz, *Synthesis*, 1972, 612.
32 F. Effenberger and G. Epple, *Angew. Chem.*, 1972, **84**, 295.
33 V. Paul, A. Sudalai, T. Daniel and K. V. Srinivasan, *Tetrahedron Lett.*, 1994, **35**, 2601.
34 J. H. Clark and D. J. Macquarrie, *Chem. Soc. Rev.*, 1996, **19**, 303.
35 G. K. Chuah, S. Jaenicke and B. K. Pong, *J. Catal.*, 1998, **175**, 80.
36 M. Scheithauer, E. Bosch, U. A. Schubert, H. Knözinger, T. K. Cheung, F. C. Jentoft, B. C. Gates and B. Tesche, *J. Catal.*, 1998, **177**, 137.
37 Z. Feng, W. S. Postula, A. Akgerman and R. G. Anthony, *Ind. Eng. Chem. Res.*, 1995, **34**, 78.
38 (*a*) S. X. Song, M. Pilko and R. A. Kydd, *Catal. Lett.*, 1998, **55**, 97; (*b*) S. X. Song and R. A. Kydd, *Catal. Lett.*, 1998, **51**, 95.
39 C. Morterra, G. Cerrato, S. DiCiero, M. Signoretto, A. Minesso, F. Pinna and G. Strukul, *Catal. Lett.*, 1997, **49**, 25.
40 K. Shimizu, N. Kounami, H. Wada, T. Shidhido and H. Hatori, *Catal. Lett.*, 1998, **54**, 153.
41 C. Morterra, G. Cerrato, F. Pinna and M. Signoretto, *J. Catal.*, 1995, **157**, 109.
42 K. Tanabe, H. Hattori and T. Yamaguchi, *Crit. Rev. Surf. Chem.*, 1990, **1**, 19.
43 T. Yamaguchi, *Appl. Catal.*, 1990, **61**, 1.
44 R. A. Comelli, C. R. Vera and J. M. Parera, *J. Catal.*, 1995, **151**, 96.

45 W. Stichert and F. Schüth, *J. Catal.*, 1998, **174**, 242.
46 A. F. Bedilo and K. J. Klabunde, *J. Catal.*, 1998, **176**, 448.
47 E. D. Egeberg and J. Engell, *Rev. Phys. Appl.*, 1989, **24**, C4.
48 C. J. Brinker and G. W. Scherer, *Sol–gel Science*, Academic Press, New York, 1990, ch. 8.
49 G. M. Pajonk, *Rev. Phys. Appl.*, 1989, **24**, C4.
50 J. I. Fukasawa and K. Tsujii, *J. Colloid Interface Sci.*, 1988, **125**, 155.
51 D. Klvana, J. Chaouki, M. Repellin-Lacroix and G. M. Pajonk, *Rev. Phys. Appl.*, 1989, **24**, C4.
52 I. Yoshida, W. Watanabe, T. Kyodo and S. Hatanaka, *Jpn. Pat. Appl. Discl. kokai*, 61-86428, May 1, 1986.
53 J. Kirchnerova, D. Klvana and J. Chaouki, *Appl. Catal. A*, 2000, **196**, 191.
54 C. Su, J. Li, D. He, Z. Cheng and Q. Zhu, *Appl. Catal. A*, 2000, **202**, 81.
55 Y. D. Tretyakov and O. A. Shlyakhtin, *J. Mater. Chem.*, 1999, **9**, 19.
56 P. D. L. Mercera, J. G. Van Ommen, E. B. M. Doesburg, A. J. Burggraaf and J. R. H. Ross, *Appl. Catal.*, 1990, **57**, 127.
57 E. P. Barrett, L. G. Joyner and P. P. Halenda, *J. Am. Chem. Soc.*, 1951, **73**, 373.
58 S. J. Gregg and K. S. W. Sing, *Adsorption, surface area and porosity*, 2nd edn., Academic Press, London, 1982.
59 K. S. W. Sing, D. H. Everett, R. A. W. Haul, L. Moscou, R. A. Pierotti, J. Rouquerol and T. Siemieniewska, *Pure Appl. Chem.*, 1985, **57**, 603.
60 H. Armendariz, B. Coq, D. Tichit, R. Dutartre and F. Figueras, *J. Catal.*, 1998, **173**, 345.
61 J. R. Sohn and H. W. Kim, *J. Mol. Catal.*, 1989, **52**, 361.
62 T. Yamaguchi, K. Tanabe and Y. C. Kung, *Mater. Chem. Phys.*, 1986, **16**, 67.
63 M. S. Scurrell, *Appl. Catal.*, 1987, **34**, 109.
64 P. D. L. Mercera, J. G. Van Ommen, E. B. M. Doesburg, A. J. Burggraaf and J. R. H. Ross, *Appl. Catal.*, 1991, **71**, 363.
65 S. Soled and G. B. McVicker, *Catal. Today*, 1992, **14**, 189.
66 J. B. Miller, S. E. Rankin and E. I. Ko, *J. Catal.*, 1994, **148**, 673.
67 B. Li and R. D. Gonzalez, *Catal. Today*, 1998, **46**, 55.
68 V. Adeeva, J. W. de Haan, J. Jänchen, G. D. Lei, V. Schünemann, L. J. M. Van de Ven, W. M. H. Sachtler and R. A. Van Santen, *J. Catal.*, 1995, **151**, 364.
69 R. S. Drago and N. Kob, *J. Phys. Chem. B*, 1997, **101**, 3360.
70 J. Thomson, G. Webb and J. M. Winfield, *J. Mol. Catal.*, 1991, **68**, 347.
71 S. E. Tung and E. McInich, *J. Catal.*, 1964, **3**, 229.
72 S. Gao and J. B. Moffat, *J. Catal.*, 1998, **180**, 142.
73 E. J. Holsstein, J. T. Wei and C. Y. Hsu, *US patent*, 4956519, 1990.
74 M. A. Coelho, D. E. Resasco, E. C. Sikabwe and R. L. White, *Catal. Lett.*, 1995, **32**, 253.
75 B. M. Choudary, M. Ravichandra-Sarma and K. Vijaya-Kumar, *J. Mol. Catal.*, 1994, **87**, 33.
76 S. Okada, K. Tanaka, Y. Nakadaira and N. Nakagawa, *Bull. Chem. Soc. Jpn.*, 1992, **65**, 2833.
77 U. Freese, F. Heinrich and F. Roessner, *Catal. Today*, 1999, **49**, 237.